Int. J. Heat Mass Transfer. Vol. 13, pp. 1177–1185. Pergamon Press 1970. Printed in Great Britain

LAMINAR FILM CONDENSATION NEAR A STAGNATION POINT ON A GENERAL CURVED SURFACE

G. POOTS and R. G. MILES
Department of Applied Mathematics, University of, Hull, England

(*Received* 9 *August* 1968 *and in revised form* 24 *November* 1969)

Abstract—The three-dimensional laminar boundary layer equations are given for laminar film condensation on a general curved surface in quiescent vapour. An example is investigated which relates to the flow in the neighbourhood of a stagnation point. Numerical results are obtained for the similarity solution in the case of condensation of steam at 100°C and atmospheric pressure. Flow and heat transfer characteristics are presented in graphical and tabular form and compared with those obtained by an approximate method.

NOMENCLATURE

$\mathbf{a}_1, \mathbf{a}_2$, unit vectors on surface S;
$\mathbf{a}_3$, unit vector normal to S;
c_p, specific heat;
f, g, h, F, G, H, velocity and thermal functions;
G_c, dimensionless group $(= gR_2^3/\nu^2)$;
h_{fg}, latent heat of condensation;
K, thermal conductivity;
$\mathbf{n}$, unit vector normal to S at the stagnation point;
Pr, Prandtl number $(= C_p\mu/K)$;
p, pressure;
R_k, principal radii of curvature, $k = 1, 2$;
T, temperature;
v_k, components of velocity, $k = 1, 2, 3$;
x_k, X_k, curvilinear co-ordinates, $k = 1, 2, 3$.

Greek symbols

δ, thickness of the condensate film;
ρ, density;
μ, viscosity;
τ_k, components of shear stress, $k = 1, 2$.

Subscripts

s, saturated;
w, wall.

Superscript

*, vapour phase.

1. INTRODUCTION

IT IS the purpose of this note to present theoretical results on laminar film condensation near a stagnation point on a general curved surface. Numerical results are obtained on investigation of the similar solution of the three-dimensional boundary layer equations for the flow of the condensate and its vapour, and are compared with those obtained by an approximate method due to Nusselt and Voskresenskiy (see Kutateladze [1]). For steam–water condensation the approximate method was found to estimate wall heat transfer and condensation rates in error by at most 5 per cent. Although this result has already been established in [2], for the two-dimensional problem of laminar film con-

densation of steam on a vertical flat plate, it was not intuitively obvious in the present three-dimensional problem which contains the interesting feature of secondary flow induced by the curvature of the surface.

2. ANALYSIS

Consider a general curved surface S maintained at temperature T_w below the saturation temperature T_s of the ambient vapour. At any point on the surface the thickness of the condensate layer is assumed thin in comparison to the principal radii of curvature so that the boundary layer approximation can be invoked. The following procedure for deriving the boundary layer equations governing the motion of the condensate and its vapour is an extension of the treatment by Howarth [3] and Rosenhead [4] for forced flow past a curved surface, and by Poots [5] for natural convection on an isothermal heated surface.

The flow of the condensate and vapour is considered to have a stagnation point located at the maximum point on the surface where the tangential plane is horizontal. This point is now chosen as the origin of curvilinear co-ordinates (x_1, x_2) on the surface. If the parametric lines $x_1 = \text{const.}$ and $x_2 = \text{const.}$ are lines of curvature of S then, within the framework of the boundary layer approximation, these are the lines of curvature of the condensate–vapour interface, S^*. Following [3–5] define $\mathbf{a}_1$ and $\mathbf{a}_2$ as unit vectors tangential to these lines, let $\mathbf{a}_3$ be the unit vector normal to S (and S^*), and x_3 be the distance measured along a normal to S in the condensate phase so that the equation of the condensate–vapour interface is denoted by

$$x_3 = \delta(x_1, x_2). \tag{1}$$

Finally let x_3^* be the distance measured along a normal to S^*.

If $\mathbf{n}$ denotes the unit vector normal (in the vertical direction) at the stagnation point and the condensate and vapour velocity fields are given by

$$\mathbf{v} = \sum_{j=1}^{3} \mathbf{a}_j v_j, \quad \mathbf{v}^* = \sum_{j=1}^{3} \mathbf{a}_j v_j^*, \tag{2}$$

the three-dimensional boundary layer equations governing laminar film condensation, given in the notation of [3–5], are obtained in component form as follows:

Condensate:

$$\frac{1}{h_1 h_2}\left\{\frac{\partial}{\partial x_1}(\rho v_1 h_2) + \frac{\partial}{\partial x_2}(\rho v_2 h_1)\right\} + \frac{\partial}{\partial x_3}(\rho v_3) = 0, \tag{3}$$

$$\rho\left\{\frac{\mathrm{D}v_1}{\mathrm{D}t} + \frac{v_1 v_2}{h_1 h_2}\frac{\partial h_1}{\partial x_2} - \frac{v_2^2}{h_1 h_2}\frac{\partial h_2}{\partial x_1}\right\} = (\rho - \rho^*)\, g\mathbf{n}\cdot\mathbf{a}_1 + \frac{\partial}{\partial x_3}\left(\mu\frac{\partial v_1}{\partial x_3}\right), \tag{4}$$

$$\rho\left\{\frac{\mathrm{D}v_2}{\mathrm{D}t} + \frac{v_1 v_2}{h_1 h_2}\frac{\partial h_2}{\partial x_1} - \frac{v_1^2}{h_1 h_2}\frac{\partial h_1}{\partial x_2}\right\} = (\rho - \rho^*)\, g\mathbf{n}\cdot\mathbf{a}_2 + \frac{\partial}{\partial x_3}\left(\mu\frac{\partial v_2}{\partial x_3}\right). \tag{5}$$

$$\rho c_p \frac{\mathrm{D}T}{\mathrm{D}t} = \frac{\partial}{\partial x_3}\left(K\frac{\partial T}{\partial x_3}\right), \tag{6}$$

where

$$\frac{\mathrm{D}}{\mathrm{D}t} = \frac{v_1}{h_1}\frac{\partial}{\partial x_1} + \frac{v_2}{h_2}\frac{\partial}{\partial x_2} + v_3\frac{\partial}{\partial x_3}.$$

Vapour: The governing equations are as given in (3)–(6) with v_j replaced by v_j^* and as the vapour is at saturation temperature T_s, ρ and μ are replaced by ρ^* and μ^*, respectively.

Boundary conditions: On the surface S

$$v_1 = v_2 = v_3 = 0, \; T = T_w. \tag{7}$$

On S^* given by $x_3^* = 0$ and $x_3 = \delta(x_1, x_2)$ the conditions for continuity in the tangential components of velocity, mass inflow and shear stress yield

$$v_1 = v_1^*, \quad v_2 = v_2^*, \quad \rho_s v_3 = \rho^* v_3^*, \quad \mu_s\frac{\partial v_1}{\partial x_3} = \mu^*\frac{\partial v_1^*}{\partial x_3^*}, \quad \mu_s\frac{\partial v_2}{\partial x_3} = \mu^*\frac{\partial v_2^*}{\partial x_3^*}; \tag{8}$$

the thermal conditions are

$$T = T_s, \qquad K_s \frac{\partial T}{\partial x_3} = -\rho^* v_3^* h_{fg}, \tag{9}$$

where h_{fg} is the latent heat of condensation. Finally in the vapour phase

$$v_1^* \to 0, \qquad v_2^* \to 0 \text{ as } x_3^* \to \infty. \tag{10}$$

The above system of equations (3)–(10) is completely defined given the condensate property relations:

$$\rho = \rho(T), \qquad c_p = c_p(T), \qquad \mu = \mu(T) \text{ and } K = K(T), \tag{11}$$

together with the specified geometry of the surface. Note that surface tension effects have been neglected. Consequently the pressure at the interface is continuous, yielding the components of the gravitational buoyancy force as stated in (4) and (5).

In the vicinity of the stagnation point the length elements h_1 and h_2 take their values at the stagnation point and consequently the scalar products become

$$\mathbf{n} \cdot \mathbf{a}_1 = \frac{h_1}{R_1} x_1, \qquad \mathbf{n} \cdot \mathbf{a}_2 = \frac{h_2}{R_2} x_2, \tag{12}$$

where R_1 and R_2 are the principal radii of curvature at the stagnation point. On substitution of (12) into the boundary layer equations a similar solution valid to first order in x_1 and x_2 is obtained.

For the condensate phase new dependent and independent dimensionless variables are introduced, namely:

$$h_1 x_1 = R_2 X_1, \quad h_2 x_2 = R_2 X_2, \quad x_3 = R_2 G_c^{-\frac{1}{4}} \eta,$$
$$\delta = R_2 G_c^{-\frac{1}{4}} \phi, \qquad v_1 = \frac{\alpha v_s}{R_2} G_c^{\frac{1}{2}} X_1 \frac{\mathrm{d}f}{\mathrm{d}\eta},$$
$$v_2 = \frac{v_s}{R_2} G_c^{\frac{1}{4}} X_2 \frac{\mathrm{d}g}{\mathrm{d}\eta},$$
$$v_3 = -\frac{v_s}{R_2} G_c^{\frac{1}{4}} (\alpha f + g)$$
$$\text{and} \quad (T - T_w)/(T_s - T_w) = h(\eta), \tag{13}$$

where $\alpha = (R_2/R_1)^{\frac{1}{2}}$ and $G_c = gR_2^3/\nu^2$. It is also convenient to introduce a further change of independent variable

$$z = \tilde{\eta}/\tilde{\phi}, \tag{14}$$

where $\tilde{\eta}$ denotes the Howarth–Dorodnitsyn variable

$$\tilde{\eta} = \int_0^{\eta} \frac{\rho}{\rho_s} \mathrm{d}\eta \quad \text{and} \quad \tilde{\phi} = \int_0^{\phi} \frac{\rho}{\rho_s} \mathrm{d}\eta, \tag{15}$$

together with the new dependent variables

$$F = \alpha f + g, \qquad G = \mathrm{d}g/\mathrm{d}z, \qquad H = h. \tag{16}$$

The boundary-layer equations now become the ordinary differential equations:

$$\left(\frac{\rho\mu}{\rho_s\mu_s} F''\right)' + \tilde{\phi}(FF'' - F'^2) + 2\tilde{\phi}(F' - G)G + (1 + \alpha^2)\tilde{\phi}^3 \frac{(\rho - \rho^*)}{\rho} = 0, \tag{17}$$

$$\left(\frac{\rho\mu}{\rho_s\mu_s} G'\right)' + \tilde{\phi}(FG' - G^2) + \tilde{\phi}^3 \frac{(\rho - \rho^*)}{\rho} = 0, \tag{18}$$

$$\left(\frac{\rho k}{\rho_s k_s} H'\right)' + \tilde{\phi}\, Pr_s \frac{c_p}{c_{p_s}} FH' = 0, \tag{19}$$

where the dash denotes differentiation with respect to z.

For the vapour phase the new independent variable is

$$z^* = G_c^{\frac{1}{4}} \frac{x_3^*}{R_2}, \tag{20}$$

and the dependent variables are:

$$v_1^* = \frac{\alpha\nu^*}{R_2} G_c^{*\frac{1}{2}} X_1 \frac{\mathrm{d}f^*}{\mathrm{d}z^*},$$
$$v_2^* = \frac{\nu^*}{R_2} G_c^{*\frac{1}{4}} X_2 \frac{\mathrm{d}g^*}{\mathrm{d}z^*},$$
$$v_3^* = \frac{\nu^*}{R_2} G_c^{\frac{1}{4}} (\alpha f^* + g^*), \tag{13*}$$

which yield the governing equations

$$F^{*'''}+F^*F^{*''}-F^{*'\,2}+2(F^{*'}-G^*)G^*=0, \quad (17^*)$$

$$G^{*''}+F^*G^{*'}-G^{*2}=0, \quad (19^*)$$

where the dash now denotes differentiation with respect to z^*, and

$$F^* = \alpha f^* + g^*, \qquad G^* = g^{*'}. \quad (16^*)$$

The boundary conditions (7)–(10) transform as follows:

$$\left.\begin{aligned} &F(0) = F'(0) = G(0) = H(0) = 0,\\ &F'(1) = \tilde{\phi}\frac{v^*}{v_s}F^{*'}(0),\\ &G(1) = \tilde{\phi}\frac{v^*}{v_s}G^*(0), \qquad F(1) = \frac{\mu^*}{\mu_s}F^*(0),\\ &F''(1) = \tilde{\phi}^2\frac{\mu^*v^*}{\mu_s v_s}F^{*''}(0),\\ &G'(1) = \tilde{\phi}^2\frac{\mu^*v^*}{\mu_s v_s}G^{*'}(0),\\ &H(1) = 1, \qquad H'(1) = \frac{h_{fg}\,Pr_s}{c_{p_s}(T_w - T_s)}\tilde{\phi}F(1), \end{aligned}\right\} \quad (21)$$

and finally

$$F^{*'}(\infty) = 0, \qquad G^*(\infty) = 0.$$

Consider now the simplification introduced by employing the Nusselt–Voskresenskiy approximate method. On neglecting the effects of convective heat transfer, inertia forces and vapour drag on the condensate flow the above nonlinear boundary value problem (17)–(19), (17*), (19*) and (21) reduces to the following:

$$\left.\begin{aligned} &\left(\frac{\rho\mu}{\rho_s\mu_s}F''\right)' = -(1+\alpha^2)\tilde{\phi}^3\frac{(\rho-\rho^*)}{\rho},\\ &\left(\frac{\rho\mu}{\rho_s\mu_s}G'\right)' = -\tilde{\phi}^3\frac{(\rho-\rho^*)}{\rho},\\ &\left(\frac{\rho k}{\rho_s k_s}H'\right)' = 0, \end{aligned}\right\} \quad (22)$$

subject to the boundary conditions:

$$F(0) = F'(0) = G(0) = H(0) = 0,$$

$$F''(1) = G'(1) = 0, \qquad H(1) = 1,$$

$$H'(1) = \frac{h_{fg}\,Pr_s\,\tilde{\phi}}{c_{p_s}(T_w - T_s)}F(1). \quad (23)$$

Note that these equations are uncoupled and this implies uncoupling of the x_1 and x_2-components of velocity. The solution of (22) and (23) is obtained following the method given in [2] and is as follows:

$$\tilde{\phi} = \frac{(1+\alpha^2)^{-\frac{1}{4}}}{\varepsilon(T_w;T_s)}\left\{\frac{Pr_s\,h_{fg}}{c_{p_s}\Delta T}\right\}^{-\frac{1}{4}}\left(\int_0^1\frac{\rho k}{\rho_s k_s}\right), \quad (24)$$

and

$$\frac{F'}{1+\alpha^2} = G = \frac{(1+\alpha^2)^{\frac{1}{4}}}{[\varepsilon(T_w;T_s)]^3}\left\{\frac{Pr_s\,h_{fg}}{c_{p_s}\Delta T}\right\}^{-\frac{1}{4}}$$

$$\times\left\{\int_0^H\frac{k\mu_s}{k_s\mu}\left(\int_{g_1=H}^{g_1=1}\frac{k}{k_s}\left(\frac{\rho-\rho^*}{\rho_s}\right)dg_1\right)dH\right\}$$

$$\times\left(\int_0^1\frac{\rho k}{\rho_s k_s}dH\right), \quad (25)$$

where

$$\varepsilon(T_w;T_s) = \left\{\int_{g_3=0}^{g_3=1}\frac{\rho k}{\rho_s k_s}\left[\int_{g_2=0}^{g_2=g_3}\frac{k\mu_s}{k_s\mu}\times\right.\right.$$

$$\left.\left.\left(\int_{g_1=g_2}^{g_1=1}\frac{k}{k_s}\left(\frac{\rho-\rho^*}{\rho_s}\right)dg_1\right)dg_2\right]dg_3\right\}. \quad (26)$$

The above integrals have already been evaluated in [2] for the condensation of steam at 100°C and atmospheric pressure. Thus approximate values for the characteristics $1/\alpha$ $(d^2f/d\eta^2)_0$, $(d^2g/d\eta^2)_0$, $(dh/d\eta)_0$, $\alpha f(\phi) + g(\phi)$ and ϕ are now available for values of the curvature parameter $\alpha = 0, \frac{1}{4}, \frac{1}{2}, \frac{3}{4}$ and 1 in the extreme case $T_w = 0$°C as displayed in Table 1. For a given α and T_w the above approximate characteristics are employed as initial starting conditions in the numerical integration for the similar solution. The iterative

Table 1. *Steam–water condensation* $T_s = 100°C$, $T_w = 0°C$, *Exact* (*E*), *Approximate* (*A*)

α	0		$\frac{1}{4}$		$\frac{1}{2}$		$\frac{3}{4}$		1	
	E	A	E	A	E	A	E	A	E	A
$f''(0)/\alpha$	0·147	0·155	0·144	0·152	0·138	0·146	0·131	0·138	0·122	0·130
$g''(0)$	0·145	0·155	0·143	0·152	0·137	0·146	0·130	0·138	0·122	0·130
$h'(0)$	1·171	1·123	1·190	1·141	1·240	1·188	1·312	1·256	1·396	1·336
ϕ	0·987	1·008	0·971	0·993	0·932	0·954	0·881	0·902	0·828	0·848
$\alpha f(\phi) + g(\phi)$	0·100	0·102	0·102	0·103	0·106	0·108	0·112	0·114	0·120	0·121
$\frac{\Delta q_{0,0}}{h_{fg}\Delta\Gamma_{0,0}}$	1·059		1·059		1·058		1·058		1·058	

procedure employed to solve (17)–(19), (17*), (19*) and (21) is described in [2] and the exact values so obtained are listed in Table 1.

3. DISCUSSION OF RESULTS

In this section the exact numerical and approximate results for steam–water condensation are compared and particular attention is paid to the effects of secondary fow.

Velocity and thermal profiles. In Figs. 1 and 2 the exact dimensionless velocity profiles $v_1/h_1x_1(g/R_2)^{\frac{1}{2}}$ and $v_2/h_2x_2(g/R_2)^{\frac{1}{2}}$ are displayed for the extreme case $T_w = 0°C$ and $\alpha = 0, \frac{1}{2}, 1$. Clearly the induced secondary flow (in the x_1-direction) does not appreciably effect the main component of flow. Moreover it is found that there is no observable variation in the direction of the velocity vector throughout the condensate and vapour layers. This occurs since the interface is in motion and the effect of vapour drag is small. In Figs. 3 and 4 exact and approximate profiles are displayed for $\alpha = \frac{1}{2}$ and $T_w = 0$ and 70°C. The approximate profiles are in error by -12 per cent in both

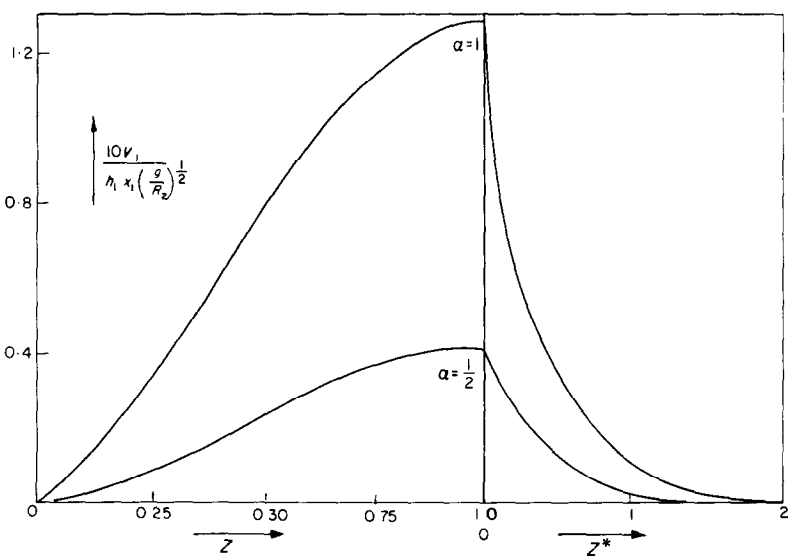

FIG. 1. Representative dimensionless velocity profiles for $T_w = 0°C$ and $\alpha = \frac{1}{2}$ and 1.

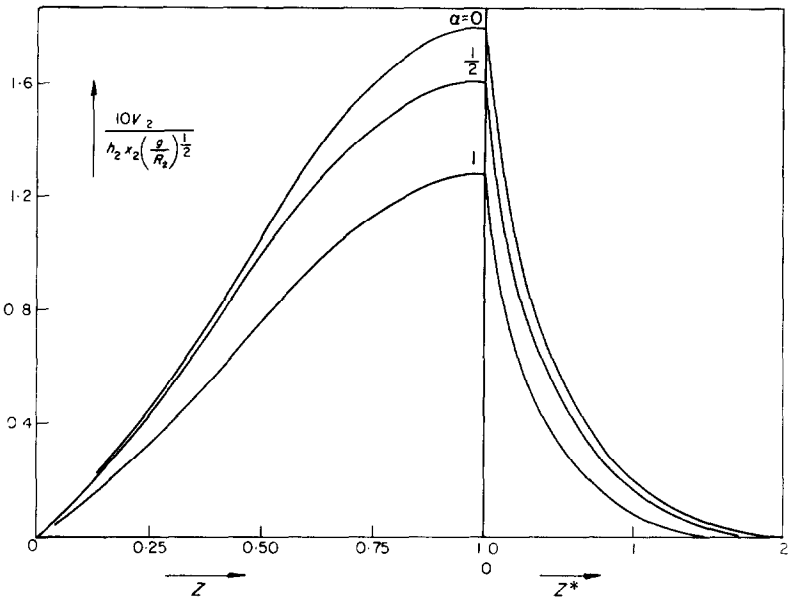

FIG. 2. Representative dimensionless velocity profiles for $T_W = 0°C$ and $\alpha = 0, \frac{1}{2}$ and 1.

the x_1 and x_2-directions and, as already discussed in [2], this is due to the neglect of vapour drag; as $(T_s - T_w) \to 0$ the error diminishes to zero. Furthermore, as in [2], the condensate thermal profile is linear and hence uninfluenced by secondary flow.

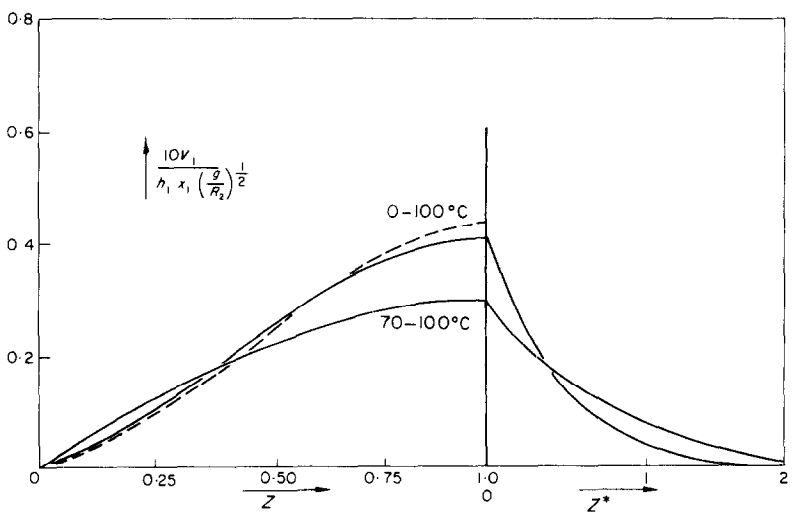

FIG. 3. Representative dimensionless velocity profiles for $\alpha = \frac{1}{2}$ and $T_W = 0$ and 70°C; Nusselt–Voskresenskiy – – –, similar solution ———.

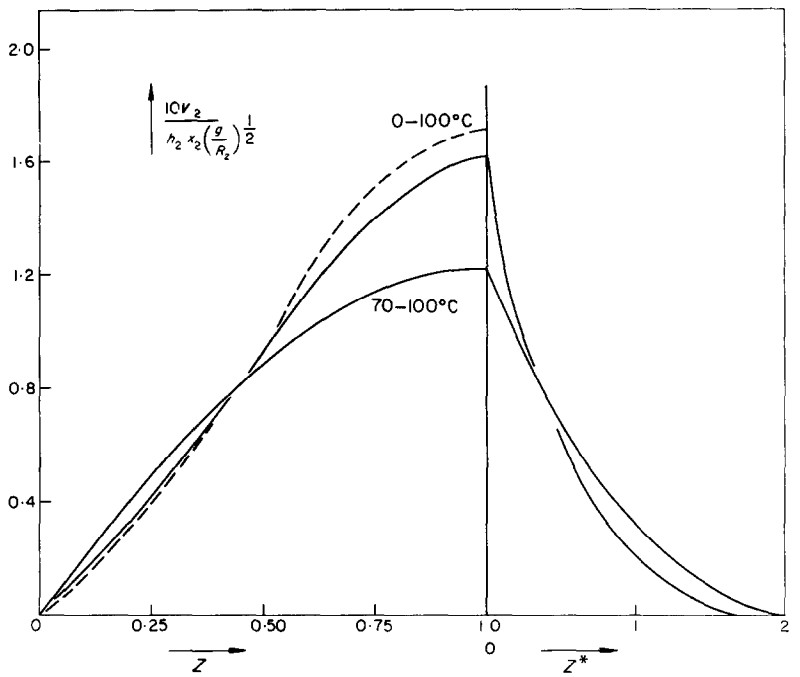

FIG. 4. Representative dimensionless velocity profiles for $T_W = 0$ and 70°C; Nusselt–Voskresenskiy – – –, similar solution ———.

Flow characteristics. Those of practical interest are as follows: First the film thickness, defined by (13) and (15), is

$$\delta = R_2 G_c^{-\frac{1}{4}} \phi. \tag{27}$$

On the basis of the boundary layer approximation the shear stress at the wall has components:

$$\tau_1 = \mu_w \left(\frac{\partial v_1}{\partial x_3}\right)_{x_3=0} = \alpha^2 \frac{v_s}{R_2} \frac{(\rho\mu)_w}{\rho_s} \frac{h_1 x_1}{R_2} G_c^{\frac{1}{4}} \frac{f''(0)}{\alpha}, \tag{28}$$

$$\tau_2 = \mu_w \left(\frac{\partial v_2}{\partial x_3}\right)_{x_3=0} = \frac{v_s}{R_2} \frac{(\rho\mu)_w}{\rho_s} \frac{h_2 x_2}{R_2} G_c^{\frac{1}{4}} g''(0). \tag{29}$$

For definitions of the condensation rate and local heat flux consider in the neighbourhood of the stagnation point a curvilinear volume element in the condensate phase with sides $h_1 dx_1$, $h_2 dx_2$ and δ lying in the $\mathbf{a}_1$, $\mathbf{a}_2$ and $\mathbf{a}_3$-directions, respectively. Thus the condensation rate $\Delta\Gamma_{0,0}$ is given by

$$\Delta\Gamma_{0,0}/h_1 h_2 \, dx_1 \, dx_2 = \rho_s (v_s)_\delta = \frac{\mu_s}{R_2} G_c^{\frac{1}{4}} [\alpha f(\phi) + g(\phi)], \tag{30}$$

and the local heat flux for the control area $h_1 h_2 \, dx_1 \, dx_2$ is

$$\Delta q_{0,0}/h_1 h_2 \, dx_1 \, dx_2 = K_w \left(\frac{\partial T}{\partial x_3}\right)_0 = \frac{\rho_w}{\rho_s} \frac{K_w \Delta T}{R_2} G_c^{\frac{1}{4}} h'(0). \tag{31}$$

It is seen from Table 1 that the Nusselt–Voskresenskiy method overestimates the condensate thickness, shear stress components and condensation rate by 2·6 and 2 per cent,

respectively. In the case of the heat flux there is an underestimation of 5 per cent. The reasons (see [2]) for these discrepancies are undoubtedly due to the neglect of vapour drag in calculation of δ, τ_1, τ_2 and $\Delta\Gamma_{0,0}$ and also the effect of the variation of conductivity with temperature in the case of the heat flux. Finally it is of interest to compare the ratio of the local heat flux to the condensation rate, namely the dimensionless group

$$\Delta q_{0,0}/h_{fg}\Delta\Gamma_{0,0} = \frac{h'(0)}{\alpha f(\phi) + g(\phi)} \frac{c_{p_s}\Delta T}{h_{fg}Pr_s} \frac{(\rho K)_w}{(\rho K)_s}. \quad (32)$$

As shown in Table 1 for $T_w = 0°C$ this ratio varies between 1·0593 and 1·0584 for the range $0 \leqslant \alpha \leqslant 1$. Thus its value is virtually independent of curvature effects. In the Nusselt–Voskresenskiy theory the ratio is unity and independent of α.

4. CONCLUSIONS

In the case of steam–water condensation at a general stagnation point it has been established that the Nusselt–Voskresenskiy method yields condensation and heat transfer rates in error by at most 5 per cent. Moreover the effect of the secondary flow induced by curvature has been satisfactorily predicted by the approximate theory. However, this would not necessarily be the case if the inertia forces and convective heat transfer were appreciable, i.e. if $Pr_w \geqslant 1$ and $(h_{fg}/c_{p_s}\Delta T) \geqslant 5$ (see [2]). Perhaps useful information could be obtained on the effects of secondary flow, and on the velocity of the Nusselt–Voskresenskiy theory by examining the condensation of a liquid metal vapour at a general stagnation point. Here the otherwise weak inertia terms would be appreciable.

REFERENCES

1. S. S. KUTATELADZE, *Fundamentals of Heat Transfer*, pp. 298–326. Edward Arnold, London (1963).
2. G. POOTS and R. G. MILES, Effects of variable physical properties on laminar film condensation of saturated steam on a vertical flat plate, *Int. J. Heat Mass Transfer* **10**, 1677–1692 (1967).
3. L. HOWARTH, The boundary layer in three-dimensional flow—Part I. Derivation of the equations for flow along a general curved surface, *Phil. Mag.* Series 7, **42**, 239–243 (1951); Part II. The flow near a stagnation point, *Phil. Mag.* Series 7, **42**, 1433–1440 (1951).
4. L. ROSENHEAD (Ed.), *Laminar Boundary Layers*, Chapter VIII. University Press, Oxford (1963).
5. G. POOTS, Laminar free convection near the lower stagnation point on an isothermal surface, *Int. J. Heat Mass Transfer* **7**, 863–879 (1964).

CONDENSATION LAMINAIRE PELLICULAIRE PRÈS D'UN POINT D'ARRÊT SUR UNE SURFACE COURBE GÉNÉRALE

Résumé—Les équations de la couche limite laminaire tridimensionnelle sont données pour la condensation laminaire pelliculaire sur une surface courbe générale dans de la vapeur au repos. Un exemple est examiné qui se rapporte à l'écoulement au voisinage d'un point d'arrêt. Les résultats numériques sont obtenus pour la solution en similitude dans le cas de la condensation de la vapeur d'eau à 100°C et à la pression atmosphérique. Les caractéristiques d'écoulement et de transport de chaleur sont présentées sous forme de graphiques et de tableaux et comparées avec celles obtenues par une méthode approchée.

LAMINARE FILMKONDENSATION NAHE EINEM STAUPUNKT

Zusammenfassung—Die dreidimensionalen Grenzschicht-Gleichungen für laminare Filmkondensation aus ruhendem Dampf an einer allgemein gekrümmten Oberfläche werden angegeben. Ein Beispiel wird untersucht, welches sich auf die Strömung in der Nähe eines Staupunktes bezieht. Numerische Ergebnisse werden erhalten für die Lösung im Fall von Kondensation von Dampf bei 100°C und 1 bar. Strömungsformen und Wärmetransportvorgänge werden in Diagrammen und Tabellen angegeben und mit Ergebnissen aus einer Näherungsmethode verglichen.

ЛАМИНАРНАЯ ПЛЕНОЧНАЯ КОНДЕНСАЦИЯ ВБЛИЗИ КРИТИЧЕСКОЙ ТОЧКИ НА ОБЫЧНОЙ КРИВОЛИНЕЙНОЙ ПОВЕРХНОСТИ

Аннотация—Приводятся уравнения для ламинарного пограничного слоя при ламинарной плёночной конденсации на обычной криволинейной поверхности в неподвижном паре. Рассматривается режим течения вблизи критической точки. Получены численные результаты для подобных решений в случае конденсации пара при 100°C и атмосферном давлении. Данные по теплообмену и гидродинамике представлены графически и сравниваются с аналогичными результатами, полученными приближенным методом.